

## Original Article

# Salvianolic acid B stimulates osteogenesis in dexamethasone-treated zebrafish larvae

Shi-ying LUO<sup>1,2</sup>, Jing-feng CHEN<sup>2</sup>, Zhi-guo ZHONG<sup>3</sup>, Xiao-hua LV<sup>2</sup>, Ya-jun YANG<sup>2</sup>, Jing-jing ZHANG<sup>3,\*</sup>, Liao CUI<sup>1,2,\*</sup>

<sup>1</sup>The State Administration of Traditional Chinese Medicine, School of Traditional Chinese Medicine, Southern Medical University, Guangzhou 510515, China; <sup>2</sup>Department of Pharmacology, Guangdong Key Laboratory for R&D of Natural Drug, Guangdong Medical University, Zhanjiang 524023, China; <sup>3</sup>Affiliated Hospital of Guangdong Medical University, Zhanjiang 524023, China

**Aim:** Our previous studies show that salvianolic acid B (Sal B) promotes osteoblast differentiation and matrix mineralization. In this study, we evaluated the protective effects of Sal B on the osteogenesis in dexamethasone (Dex)-treated larval zebrafish, and elucidated the underlying mechanisms.

**Methods:** At 3 d post fertilization, wild-type AB zebrafish larvae or bone transgenic tg (*sp7:egfp*) zebrafish larvae were exposed to Sal B, Dex, or a mixture of Dex+Sal B for 6 d. Bone mineralization in AB strain larval zebrafish was assessed with alizarin red staining, and osteoblast differentiation in tg (*sp7:egfp*) larval zebrafish was examined with fluorescence scanning. The expression of osteoblast-specific genes in the larvae was detected using qRT-PCR assay. The levels of oxidative stress markers (ROS and MDA) in the larvae were also measured.

**Results:** Exposure to Dex (5–20  $\mu\text{mol/L}$ ) dose-dependently decreased the bone mineralization area and integral optical density (IOD) in wild-type AB zebrafish larvae and the osteoblast fluorescence area and IOD in tg (*sp7:egfp*) zebrafish larvae. Exposure to Dex (10  $\mu\text{mol/L}$ ) significantly reduced the expression of osteoblast-specific genes, including *runx2a*, osteocalcin (OC), alkaline phosphatase (ALP) and *osterix* (*sp7*), and increased the accumulation of ROS and MDA in the larvae. Co-exposure to Sal B (0.2–2  $\mu\text{mol/L}$ ) dose-dependently increased the bone mineralization area and IOD in AB zebrafish larvae and osteoblast fluorescence in tg (*sp7:egfp*) zebrafish larvae. Co-exposure to Sal B (2  $\mu\text{mol/L}$ ) significantly attenuated deleterious alterations in bony tissue and oxidative stress in both Dex-treated AB zebrafish larvae and tg (*sp7:egfp*) zebrafish larvae.

**Conclusion:** Sal B stimulates bone formation and rescues GC-caused inhibition on osteogenesis in larval zebrafish by counteracting oxidative stress and increasing the expression of osteoblast-specific genes. Thus, Sal B may have protective effects on bone loss triggered by GC.

**Keywords:** salvianolic acid B; polyphenol; glucocorticoid; osteoporosis; osteogenesis; oxidative stress; zebrafish

Acta Pharmacologica Sinica (2016) 37: 1370–1380; doi: 10.1038/aps.2016.62; published online 29 Aug 2016

## Introduction

Extensive evidence demonstrates that glucocorticoid (GC) excess decreases osteoblast differentiation and functions, as well as increases apoptosis of osteoblast and osteocytes. This ultimately leads to osteoporosis characterized by the inhibition of bone formation, named glucocorticoid-induced osteoporosis (GIO)<sup>[1,2]</sup>. However, the underlying mechanisms of these deleterious effects caused by GC on skeletal tissue remain unclear, and there are also no ideal drugs and methods suitable for GIO.

Recently, epidemiological and genetic studies on both

humans and rodents show that the accumulation of reactive oxygen species (ROS) and enhancement of oxidative stress (OS) play a pivotal role in the development of osteoporosis<sup>[3–5]</sup>. In skeletal tissue, excessive ROS generation directly promotes apoptosis of osteoblasts and osteocytes<sup>[6–8]</sup>, and ROS-elicited OS also contributes to increased osteoclast differentiation and function<sup>[9,10]</sup>. Furthermore, studies confirm that GC elicits increased ROS production and subsequent OS in skeletal tissue<sup>[11–13]</sup>. These studies indicate that excessive GC may significantly contribute to bone loss, partially due to oxidative stress, and antioxidant treatment may counteract GC-induced osteopenia and osteoporosis.

Salvianolic acid B (Sal B, or lithospermic acid B), the major aqueous bioactive component of *Salvia miltiorrhiza Bunge*, is widely used clinically in China as the main pharmacological ingredient of approved *Salvia miltiorrhiza* agents for cardio-

\*To whom correspondence should be addressed.

E-mail jingjing.zhang@live.com (Jing-jing ZHANG);  
cuiliao@163.com (Liao CUI)

Received 2016-01-30 Accepted 2016-05-10

cerebral vascular diseases. As a polyphenolic acid compound with seven phenolic hydroxyl groups, Sal B is one of the strongest natural antioxidants<sup>[14, 15]</sup> and is metabolized *in vivo* into tanshinol, another aqueous bioactive ingredient of *Salvia miltiorrhiza* and a strong natural antioxidant containing two phenolic hydroxyl groups (Figure 1). Interestingly, our previous studies demonstrated that both Sal B and tanshinol promoted osteoblastic differentiation and functions *in vitro*, and the aqueous extracts of *Salvia miltiorrhiza*, of which the major components are Sal B and tanshinol, effectively prevented osteopenia in rats treated with long-term excessive prednisone<sup>[16-18]</sup>.

*Danio rerio* (zebrafish) is a powerful whole *in vivo* animal model for bone study and drug screening because of its many advantages<sup>[19, 20]</sup>. Since 2006, when Fleming *et al*<sup>[21]</sup> found that wild-type larval zebrafish exposed to prednisolone showed an obvious delay of skull mineralization based on alizarin red staining, zebrafish larvae have been widely used for the high-throughput screen for anti-osteoporotic candidates<sup>[22, 23]</sup>. Tg (*sp7:egfp*) is a transgenic line zebrafish characterized by the osterix gene driven expression of green fluorescent protein (GFP) in osteoblast differentiation<sup>[24, 25]</sup>. Because GFP-positive osteoblasts are visible in tg(*sp7:egfp*) larvae, the process of osteoblast differentiation and bone formation can be directly monitored via alteration of GFP fluorescence intensity using a fluorescence microscope.

Based on the above, we elucidated the preventive effects of Sal B on the inhibition of bone formation induced by exces-

sive GC in both wild-type AB strain zebrafish larvae and bone transgenic juvenile zebrafish-tg(*sp7:egfp*) and further investigated the underlying mechanism in this study.

## Materials and methods

### Zebrafish husbandry

Zebrafish of the AB wild line and bone transgenic *osterix:nlsGFP* line, named tg(*sp7:egfp*)<sup>[26]</sup>, were used. The embryos of the AB line and tg(*sp7:egfp*) line zebrafish were, respectively, collected from the natural mating and spawning of wild-type AB line zebrafish and tg(*sp7:egfp*) transgenic zebrafish. At 36 h post fertilization, the embryos with green fluorescence, considered tg(*sp7:egfp*), were identified and selected under a fluorescence microscope. Both the embryos and larvae of the AB strain and tg(*sp7:egfp*) were reared in egg water (5 mmol/L NaCl, 0.17 mmol/L KCl, 0.4 mmol/L CaCl<sub>2</sub>, 0.16 mmol/L MgSO<sub>4</sub>, and 10 ppm methylene blue) containing 30 ppm *N*-phenylthiourea and in egg water without *N*-phenylthiourea under standard conditions, respectively<sup>[27]</sup>.

### Preparations of compound solution

Dexamethasone (Dex, MP, USA) and Calcitriol Soft Capsule (rocalirol; Roche, Switzerland) were solubilized in dimethyl sulfoxide (DMSO, Sigma-Aldrich, Japan) and stored at -20°C. The stock solution concentrations of Dex and rocalirol were 10 mmol/L and 6×10<sup>-4</sup> μg/mL, respectively. Sal B (Tianjingshilang, China; Sal B content 90%) was dissolved and diluted to 10 mmol/L in egg water before use.

### Compound treatment in 24-well plates

Zebrafish larvae at 3 d post fertilization (dpf) were transferred into 24-well plates containing egg water. Compound treatment was performed in 24-well plates with 6 larvae per well. After being dissolved, the stock solution of each compound was diluted into egg water and added into 24-well plates. The final volumes of medium per well were adjusted to 1 mL. From 3 dpf to 9 dpf, half the medium in each well was replaced with fresh solution every 24 h. At 9 dpf, larvae were collected and fixed for bone tissue alizarin red staining or fluorescence imaging as described.

### Measurement of osteogenesis in intact zebrafish larvae exposed to Dex

The AB wild-strain or tg(*sp7:egfp*) line zebrafish larvae were randomly divided into various treatment groups (*n*=12 larvae/2 wells per group). Larvae were exposed to different concentrations of Dex (5, 10, 15, and 20 μmol/L) from 3 dpf to 9 dpf, and 0.1% DMSO was the vehicle control treatment. At 9 dpf, zebrafish larvae were collected. The AB wild strain underwent alizarin red staining and bone mineralization quantitative analysis as described. The tg(*sp7:egfp*) line underwent fluorescence scanning and fluorescence picture quantitative analysis using laser scanning confocal microscope (LSCM) and Image-Pro Plus image analysis software version 6.0 (IPP 6.0), respectively, as described.

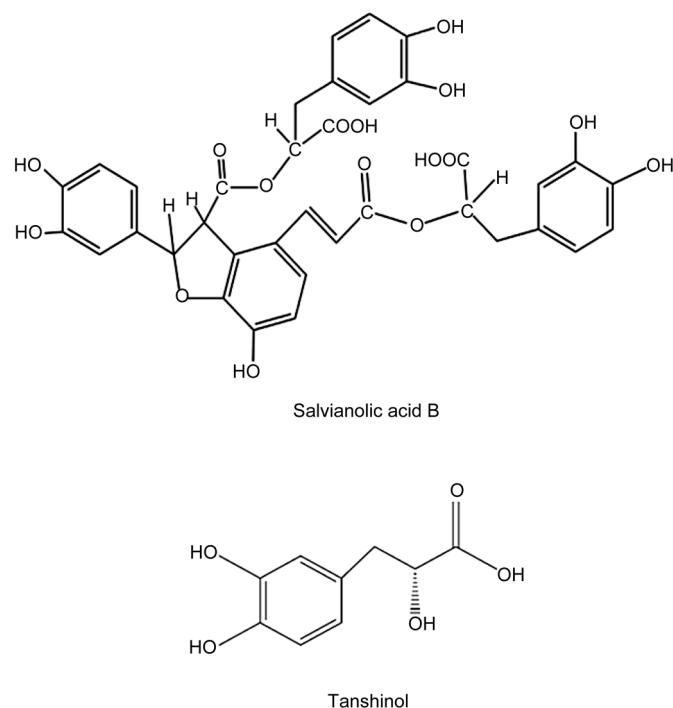


**Figure 1.** Chemical structure of salvianolic acid B and tanshinol. Salvianolic acid B contains seven phenolic hydroxyl groups, tanshinol two phenolic hydroxyl groups. Three molecules of tanshinol and a molecule of caffeic acid constitute a molecule of salvianolic acid B.

### Determination of osteogenesis in intact zebrafish larvae treated with Sal B

As described in the method as above, zebrafish larvae were treated with different concentrations of Sal B (0.2, 0.5, 1.0, and 2.0  $\mu\text{mol/L}$ ) from 3 dpf to 9 dpf, and egg water was used as the control treatment ( $n=12$  larvae/2 wells per group). At the end of experiment, alizarin red staining and fluorescence scanning were performed.

### Assay of bone formation in zebrafish larvae treated with Dex in the presence of Sal B

Based on the results of Dex on osteogenesis in intact zebrafish larvae, Dex at the dose of 10  $\mu\text{mol/L}$  was used in subsequent experiments. Zebrafish larvae were divided into 9 groups ( $n=12$  larvae/2 wells/group). Both the AB wild strain and *tg(sp7:egfp)* line zebrafish larvae were treated with 0.1% DMSO (vehicle control), 10  $\mu\text{mol/L}$  Dex, 10  $\mu\text{mol/L}$  Dex+Sal B (0.2, 0.5, 1.0, 2.0, 4.0, and 10  $\mu\text{mol/L}$ ), or 10  $\mu\text{mol/L}$  Dex+ $6\times 10^{-6}$   $\mu\text{g/mL}$  rocalirol (positive control) from 3 dpf to 9 dpf. The rocalirol  $6\times 10^{-6}$   $\mu\text{g/mL}$  group was the positive control group for Sal B in terms of attenuating Dex-induced inhibition of bone formation. At the end of the experiment, alizarin red staining and fluorescence scanning were performed.

### Expression of genes related to osteogenesis and oxidative stress in zebrafish larvae

According to the experimental results of Sal B on bone formation in zebrafish treated with Dex, Sal B at the dose of 2  $\mu\text{mol/L}$  was used in the following tests. The AB strain zebrafish larvae at 3 dpf were reared 30 per well in 6-well plates with egg water, divided into the following groups, and exposed to the corresponding compounds for 6 days ( $n=90$  larvae/3 well per group): vehicle control (0.1% DMSO); 10  $\mu\text{mol/L}$  Dex; and 10  $\mu\text{mol/L}$  Dex+2  $\mu\text{mol/L}$  Sal B. The total volume of medium per well was 5 mL, and half the medium of each well was changed every day. At 9 dpf, larvae were collected and subjected to qRT-PCR assay ( $n=10$  larvae/group) and oxidative stress assay ( $n=80$  larvae/group).

### Alizarin red staining of bone tissue and quantitative analysis of bone mineralization

At 9 dpf, the AB strain zebrafish were fixed in a 4% paraformaldehyde solution for 2 h. The protocol for bone alizarin red staining was adapted from that described in previous reports<sup>[28]</sup>. In short, larvae were dehydrated in 50% ethanol-PBS for 10 min and subsequently stained with 0.1% alizarin red (MP, USA) in 0.5% KOH overnight. After washes in ultrapure water, larvae were bleached in 1.5%  $\text{H}_2\text{O}_2$ -1% KOH for 30 min. Next, destaining was performed with different proportions of mixtures of 0.5% KOH-glycerol (3:1, 1:1, 1:3), and zebrafish samples were stored in 100% glycerol at 4°C.

The method for the quantitation of head bone mineralization was the same as that previously described<sup>[29]</sup>. Larval zebrafish were placed and fixed on a glass slide with 100% glycerol, and the dorsal aspect head bone was visualized and photographed using a M205 FA stereo microscope (Leica, Ger-

many) equipped with a DFC310 FX camera (Leica, Germany). All images for each test were taken under identical conditions. The images were analyzed using Image-Pro Plus image analysis software version 6.0 (IPP 6.0, Media Cybernetics, USA), and the areas and integral optical density (IOD) of alizarin red staining were quantified. At least ten zebrafish in each group were stained with alizarin red for mineralization analysis.

### LSCM scans and fluorescence imaging quantitative analysis

At 9 dpf, *tg(sp7:egfp)* zebrafish were fixed in 4% paraformaldehyde solution for 2 h and stored in PBS at 4°C. The head of the larvae was separated and transferred to confocal laser special glass-bottom dishes. Keeping the dorsal aspect of the head up, the head was wrapped in 1% low-melting agarose gel and scanned with a TCS SP5II LSCM (Leica, Germany). Each sample was scanned for 10 layers. The fluorescence images for GFP of the head bone were excited at 488 nm, with emission from 500 to 550 nm, and were recorded at high resolution (1024 pixels square). High-resolution confocal fluorescence images were analyzed using IPP 6.0 (Media Cybernetics, USA). Fluorescence images were converted to grayscale images, and the fluorescence intensity was converted to a gray value. An intensity range was set to include all gray localizations, and the area and the density of this gray localization were calculated. The same intensity range was applied to all images of larvae. More than ten pieces of zebrafish were used for each group.

### qRT-PCR assay

Total RNA from wild-type AB strain zebrafish larvae ( $n=10$  larvae/group) were extracted using Trizol reagent according to the reagent manufacturer's instructions (Abcam, USA). The cDNA was synthesized using SuperScript II reverse transcriptase (Invitrogen, USA). The qRT-PCR of osteoblast-specific genes (*runx2a*, *ALP*, *OC*, and *sp7*) was performed using a Roche Light Cycler 480 QPCR System (Roche, Switzerland), and the primer sequences of these genes and housekeeping genes ( $\beta$ -actin) are listed in Table 1. The data were analyzed using the accompanying Opticon Monitor software. PCR assays for each gene were performed in triplicate.

**Table 1.** Primer sequences for qRT-PCR.

mRNA	Forward sequence (5'-3')	Reverse sequence (5'-3')
<i>runx2a</i>	GACTCCGACCTCACGACAA	CGTCCCGTCAGGAACATC
<i>sp7</i>	AAGAAACCTGTCCACAGCTG	GAGGCTTTACCGTACACCTT
<i>ALP</i>	CAGTGGGAATCGTCACAACAA	CCACACAGTGGGCATAAGCA
<i>OC</i>	TGGCCTCTATCATCATGAGACAGA	CTCTCGAGCTGAAATGGAGTCA
$\beta$ -Actin	CAACAGGGAAAAGATGACACAGAT	CAGCCTGGATGGCAACGT

### Oxidative stress analysis

The levels of ROS and malonic dialdehyde (MDA) and the activity of superoxide dismutase (SOD), glutathione peroxi-

dase (GSH) and hydrogen peroxidase (catalase, CAT), respectively, reflect the oxidation and antioxidant levels of the body. Briefly, zebrafish larvae ( $n=80$  larvae/group) were washed twice using ultrapure water and then homogenized in 500  $\mu$ L of ultrapure water with a glass homogenizer. The homogenate was centrifugalized, and the supernatant was collected and used for tests. ROS was measured using an oxidation-sensitive fluorescent probe dye (DCFH-DA) chemical reagent kit (Beyotime Institute of Biotechnology, China), and the other indices of oxidative stress above were determined using chemical colorimetry according to the reagent manufacturer's instructions (Nanjing Jiancheng Bioengineering Institute, China).

### Statistical analysis

Data were analyzed using SPSS version 16.0 (SPSS Inc, Chicago, IL, USA). If the data were normally distributed and had an equivalency of variances, one-way analysis of variance (ANOVA) with Fisher's PLSD test was used to test the statistical differences among various treatments. Otherwise, Dunn's method for *post hoc* test was used to perform pairwise comparisons of treatment groups. If probabilities are less than 0.05 ( $P<0.05$ ), statistical differences are considered significant. Data for all parameters are presented as the mean $\pm$ SD or the mean $\pm$ SEM.

## Results

### Dex inhibits osteoblast differentiation and reduces mineralized matrix in intact larval zebrafish skull

To clarify the influence of glucocorticoid on bone formation in an earlier vertebrate model, such as zebrafish, larval zebrafish were exposed to different concentrations of Dex. Compared to the vehicle control, there was a significant decrease in the area and IOD of skull green fluorescence in tg(*sp7:egfp*) zebrafish larvae treated with Dex at concentrations ranging from 5 to 20  $\mu$ mol/L ( $P<0.05$ ), and they showed a dose-dependent decrease with increasing concentrations of Dex (Figure 2). The osterix gene (*sp7*) is a pivotal and necessary regulatory factor during osteoblast differentiation. Tg(*sp7:egfp*) is a transgenic line zebrafish characterized by osterix gene driven expression of green fluorescent protein (GFP) during osteoblast differentiation. The osteoblasts of tg(*sp7:egfp*) are selectively marked with GFP, and the area and IOD of green fluorescence directly reflects the osteoblast differentiation and amount. Dex at concentrations from 5 to 20  $\mu$ mol/L also decreased the area and IOD of the skull mineralized matrix stained with alizarin red in the AB strain larval zebrafish in a dose-dependent manner ( $P<0.05$ ) (Figure 3). These results suggest that Dex caused a dose-dependent decrease of mineralized matrix and osteoblast differentiation in zebrafish larvae. However, Dex at concentrations of 15 and 20  $\mu$ mol/L also markedly reduced the

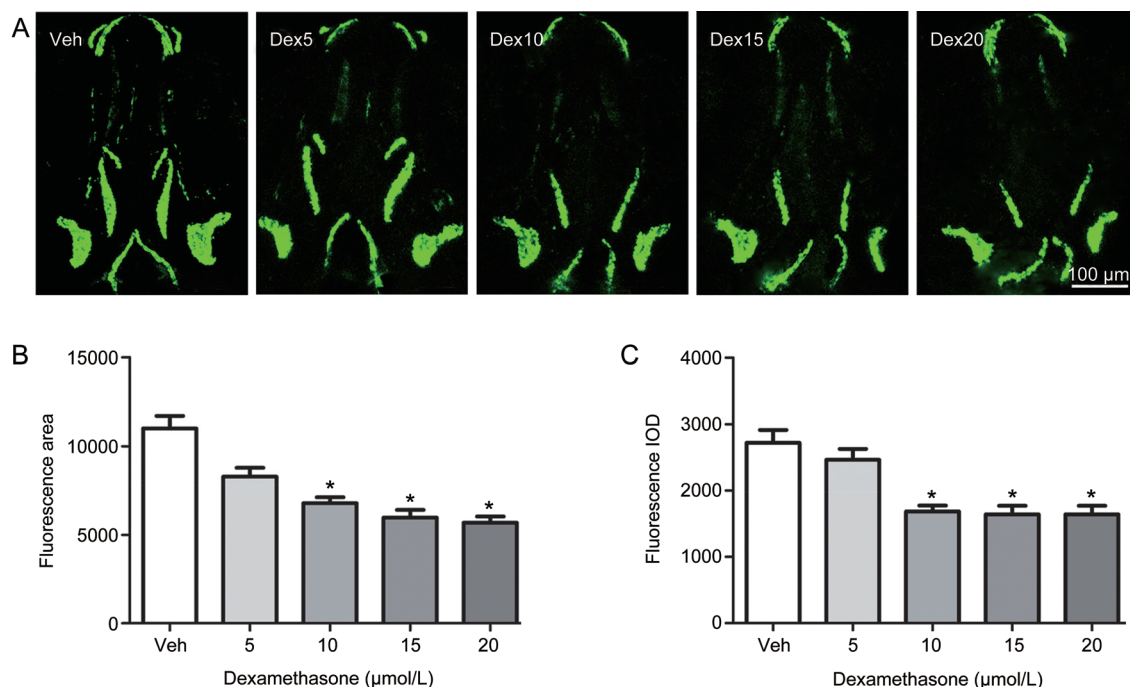


**Figure 2.** Dex treatment leads to decreased osteoblast differentiation of skull in tg(*sp7:egfp*) larval zebrafish. (A) Green fluorescence images of skull dorsal aspect using LSCM in tg(*sp7:egfp*) larval zebrafish at 9 dpf exposed to 0, 5, 10, 15, and 20  $\mu$ mol/L Dex for 6 d; (B) The influence of Dex on skull green fluorescence area analyzed by IPP6.0 in 9-dpf tg(*sp7:egfp*) larval zebrafish and (C) The influence of Dex on skull green fluorescence IOD analyzed by IPP6.0 in 9 dpf tg(*sp7:egfp*) larval zebrafish. Notes: LSCM (laser scanning confocal microscopy); IPP6.0 (Image-Pro Plus image analysis software version 6.0); IOD (integral optical density); Veh (vehicle control, 0.1% dimethyl sulphoxide); Dex5 (Dex 5  $\mu$ mol/L); Dex10 (Dex 10  $\mu$ mol/L); Dex15 (Dex 15  $\mu$ mol/L); Dex20 (Dex 20  $\mu$ mol/L). Data are given as mean $\pm$ SD.  $n\geq 9$ . \* $P<0.05$  vs vehicle control.

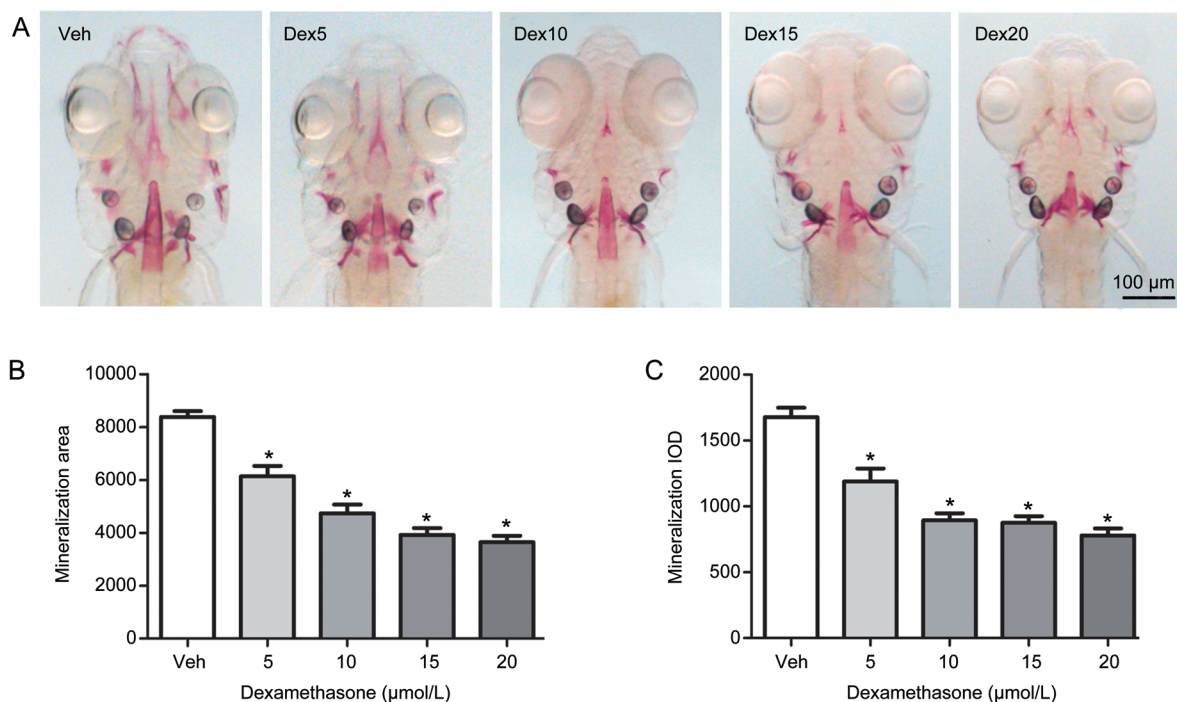


**Figure 3.** Dex treatment leads to decreased mineralized matrix of skull in AB strain larval zebrafish. (A) Images of skull dorsal aspect of alizarin red stained AB strain larval zebrafish at 9 dpf exposed to 0, 5, 10, 15, and 20  $\mu\text{mol/L}$  Dex for 6 d; (B) The influence of Dex on skull mineralization area analyzed by IPP6.0 in 9 dpf AB strain larval zebrafish; (C) The influence of Dex on skull mineralization IOD analyzed by IPP6.0 in 9 dpf AB strain larval zebrafish. Notes: IPP6.0 (Image-Pro Plus image analysis software version 6.0); IOD (integral optical density); Veh (vehicle control, 0.1% dimethyl sulphoxide); Dex5 (Dex 5  $\mu\text{mol/L}$ ); Dex10 (Dex 10  $\mu\text{mol/L}$ ); Dex15 (Dex 15  $\mu\text{mol/L}$ ); Dex20 (Dex 20  $\mu\text{mol/L}$ ). Data are given as mean $\pm$ SD.  $n\geq 9$ . \* $P<0.05$  vs vehicle control.

swimming activity of the fish and even led to death in larval zebrafish (data not shown). Based on the above results, Dex at 10  $\mu\text{mol/L}$  was used in the following experiment.

#### Sal B stimulates osteoblast differentiation and increases mineralization of the skull of larval zebrafish

To assess the benefit of Sal B on bone formation, zebrafish larvae were exposed to different concentrations of Sal B. As shown in Figure 4, Sal B significantly increased the area and IOD of the green fluorescence of the skull at concentrations of 0.5 to 2.0  $\mu\text{mol/L}$  in *tg(sp7:egfp)* zebrafish larvae compared to the control ( $P<0.05$ ). However, different concentrations of Sal B, from 0.5 to 2.0  $\mu\text{mol/L}$ , increased the area and IOD of green fluorescence to the same extent. Sal B (0.5, 1, and 2.0  $\mu\text{mol/L}$ ) also increased the area of the skull stained with alizarin red and the staining intensity in zebrafish larvae compared to the control ( $P<0.05$ ). Furthermore, the effects of the different concentrations on increasing the area and IOD of the skull stained with alizarin red were identical (Figure 5). No effect in zebrafish larvae was observed with a lower concentration of Sal B at 0.2  $\mu\text{mol/L}$ . These results indicate that during the early development of zebrafish skull, Sal B can promote bone formation by stimulating osteoblast differentiation and bone mineralization.

#### Sal B attenuates Dex-induced inhibition of osteoblast differentiation and mineralization in the skull of zebrafish larvae

Because Sal B can promote bone formation during early development of the zebrafish skull, we determined whether Sal B may also attenuate the deleterious effect of GC on bone formation in larval zebrafish. From 3 dpf to 9 dpf, zebrafish larvae were exposed to 10  $\mu\text{mol/L}$  Dex alone or a mixture of 10  $\mu\text{mol/L}$  Dex and different concentrations of Sal B ranging from 0.2 to 10  $\mu\text{mol/L}$ . As shown in Figure 6, Sal B at concentrations from 0.5 to 10  $\mu\text{mol/L}$  attenuated the decrease in the area and IOD of alizarin red staining in the skull of larval zebrafish triggered by 10  $\mu\text{mol/L}$  Dex ( $P<0.05$ ), particularly at 2  $\mu\text{mol/L}$ . Treatment with Sal B at concentrations from 0.5 to 10  $\mu\text{mol/L}$  also rescued 10  $\mu\text{mol/L}$  Dex-induced reduction of the green fluorescence area and IOD in *tg(sp7:egfp)* zebrafish larvae ( $P<0.05$ ). The strongest rescue effect of Sal B occurred for 2  $\mu\text{mol/L}$  (Figure 7), which is consistent with the results of the alizarin red-stained zebrafish larvae. As a positive control, rocalirol also hampered the decrease in the area and IOD of alizarin red staining and green fluorescence caused by GC. Sal B at 2  $\mu\text{mol/L}$  and rocalirol show the same effect of attenuating the Dex-induced inhibition of osteoblast differentiation and bone mineralization in larval zebrafish. These results suggest that Sal B rescues Dex-induced inhibition of bone forma-

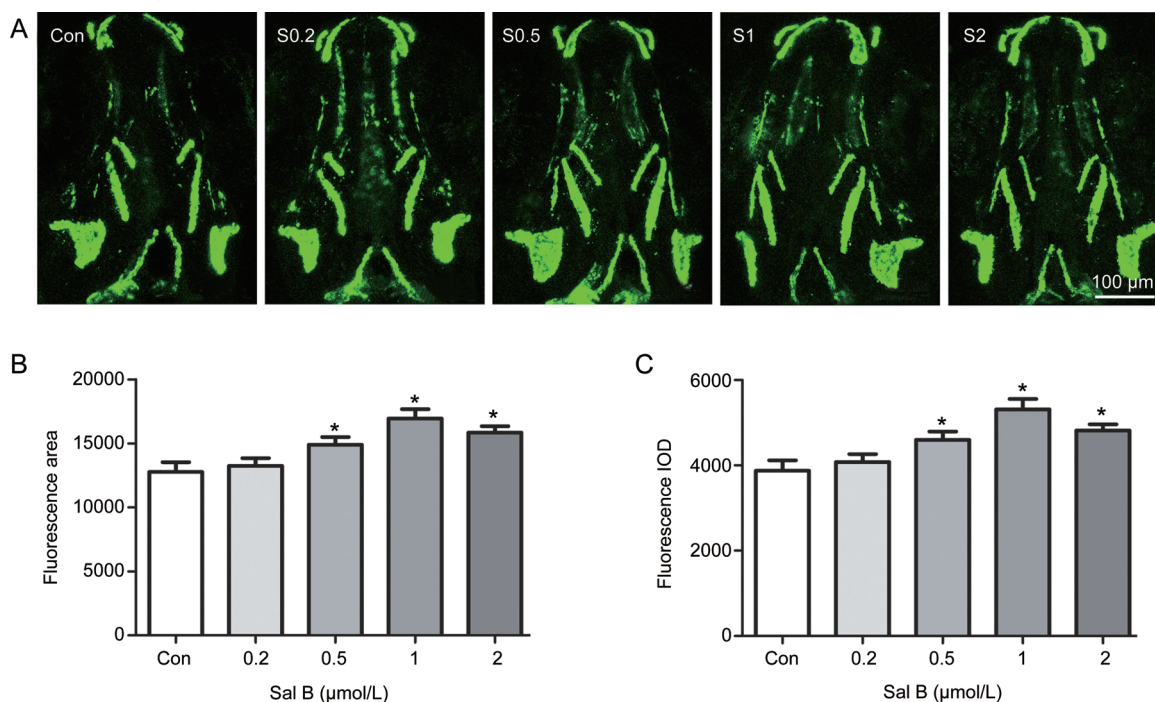


**Figure 4.** Salviaolic acid B stimulates skull osteoblast differentiation in *tg(sp7:egfp)* larval zebrafish. (A) Green fluorescence images of skull dorsal aspect using LSCM in *tg(sp7:egfp)* larval zebrafish at 9-dpf treated with 0, 0.2, 0.5, 1, and 2  $\mu\text{mol/L}$  Sal B for 6 d; (B) the influence of Sal B on skull green fluorescence area analyzed by IPP6.0 in 9-dpf *tg(sp7:egfp)* larval zebrafish and (C) the influence of Sal B on skull green fluorescence IOD analyzed by IPP6.0 in 9-dpf *tg(sp7:egfp)* larval zebrafish. Notes: LSCM (laser scanning confocal microscopy); IPP6.0 (Image-Pro Plus image analysis software version 6.0); IOD (integral optical density); Con (control, egg water); S0.2 (Sal B 0.2  $\mu\text{mol/L}$ ); S0.5 (Sal B 0.5  $\mu\text{mol/L}$ ); S1 (Sal B 1  $\mu\text{mol/L}$ ); S2 (Sal B 2  $\mu\text{mol/L}$ ). Data are given as mean  $\pm$  SD.  $n \geq 9$ . \* $P < 0.05$  vs vehicle control.

tion in zebrafish larvae by stimulating osteoblast differentiation and bone mineralization. Based on the above data, Sal B at 2  $\mu\text{mol/L}$  was used in the following study.

#### Expression of osteoblast-specific genes is down-regulated by Dex in zebrafish and is rescued by Sal B

To further confirm the protective effect of Sal B on osteogenesis under conditions of GC treatment, a quantitative real-time PCR assay was performed to ascertain alterations in the expression of osteoblast-specific genes in larval zebrafish, including *runx2a*, *osteocalcin (OC)*, *alkaline phosphatase (ALP)* and *osterix (sp7)*. As shown in Figure 8, compared to the corresponding control, the mRNA expression of *runx2a*, *OC*, *ALP* and *sp7* was significantly reduced in zebrafish larvae treated with 10  $\mu\text{mol/L}$  Dex. Conversely, Sal B rescued the Dex-induced down-regulation of osteoblast-specific genes. These results further demonstrate that Sal B rescues the Dex-induced inhibition of osteogenesis by up-regulating the expression of osteoblast-specific genes.

#### Sal B attenuates Dex-induced oxidative stress in zebrafish

As shown in Figure 9, compared to the vehicle control, the level of ROS determined using an oxidation-sensitive fluorescent probe dye, DCFH-DA, was significantly increased in 10  $\mu\text{mol/L}$  Dex-treated larvae, based on the increase of the malonic dialdehyde (MDA) level (Figure 9A and 9B). Moreover,

in larval zebrafish exposed to Dex, the activities of superoxide dismutase (SOD), glutathione peroxidase (GSH) and hydrogen peroxidase (CAT) showed obvious decreases. Furthermore, compared to the 10  $\mu\text{mol/L}$  Dex-treatment, 2  $\mu\text{mol/L}$  Sal B decreased the levels of ROS and MDA. Furthermore, the changes of antioxidants, including SOD, GSH and CAT were not significantly different (Figure 9C, 9D, and 9E). These results indicate that Dex stimulates the generation of ROS and enhances oxidative stress, which can be reduced by Sal B in zebrafish larvae.

#### Discussion

It has been reported that zebrafish is highly conserved in terms of bone architecture and bone metabolism regulation compared to humans<sup>[30, 31]</sup>. Evidence shows that the zebrafish skull develops from 3 dpf to 9 dpf by endochondral and intramembranous ossification, which is similar to the osteogenesis mechanism of humans<sup>[32]</sup>. The early-stage zebrafish larvae skull, which contains both osteoblasts and osteoclasts, is a complete system of bone formation and bone resorption<sup>[33, 34]</sup>. Osteoblast differentiation and proliferation lead to bone formation, and osteoclastogenesis occurs at the same time, highly similar to that in mammals. Our results showed that the skull of 9 dpf AB zebrafish larvae was stained red with alizarin red, indicating that mineralized skull had been formed in 9 dpf larval zebrafish. Our results are consistent with the litera-

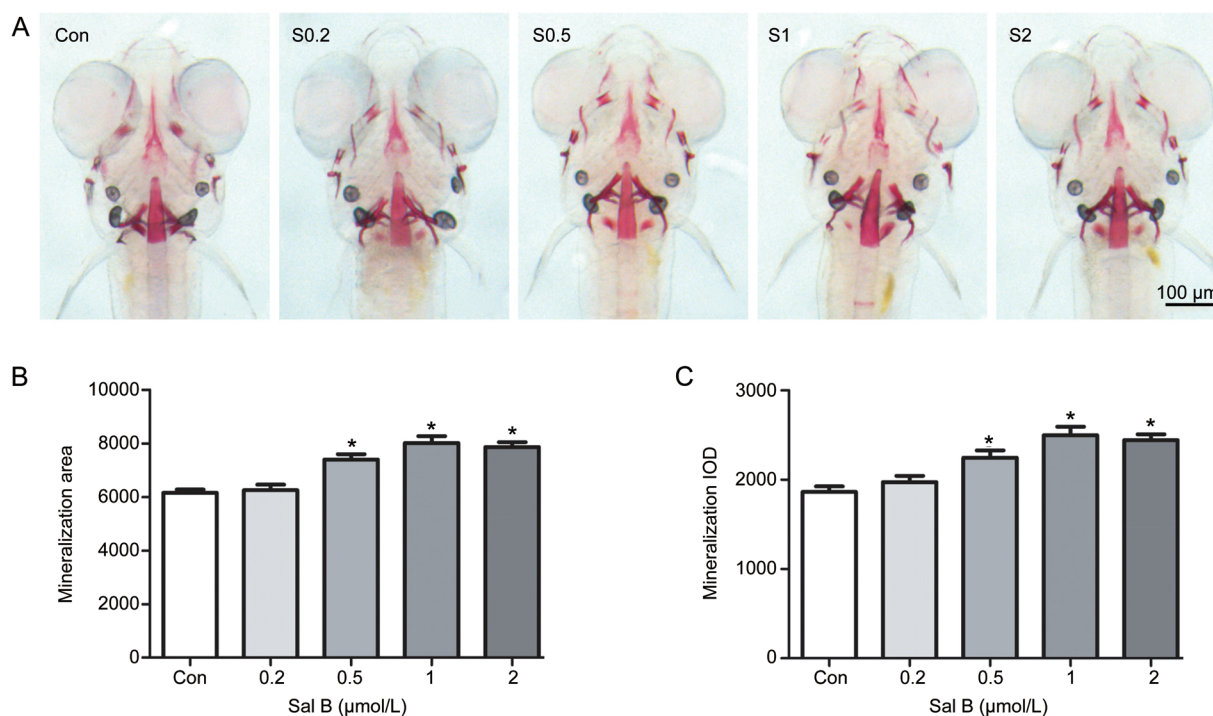


**Figure 5.** Salviaolic acid B increases skull mineralized matrix in intact AB strain larval zebrafish. (A) Images of skull dorsal aspect of alizarin red stained AB strain larval zebrafish at 9 dpf treated with 0, 0.2, 0.5, 1, and 2  $\mu\text{mol/L}$  Sal B for 6 d; (B) the influence of Sal B on skull mineralization area analyzed by IPP6.0 in 9-dpf AB strain larval zebrafish and (C) the influence of Sal B on skull mineralization IOD analyzed by IPP6.0 in 9-dpf AB strain larval zebrafish. Notes: IPP6.0 (Image-Pro Plus image analysis software version 6.0); IOD (integral optical density); Con (control, egg water); S0.2 (Sal B 0.2  $\mu\text{mol/L}$ ); S0.5 (Sal B 0.5  $\mu\text{mol/L}$ ); S1 (Sal B 1  $\mu\text{mol/L}$ ); S2 (Sal B 2  $\mu\text{mol/L}$ ). Data are given as mean  $\pm$  SD.  $n \geq 9$ . \* $P < 0.05$  vs vehicle control.

ture. Alizarin red staining in tiny larva is a fine and complicated procedure, and it only reflects bone mineralization. In *tg(sp7:egfp)*, osteoblasts are specifically marked by GFP, which make osteoblasts visible<sup>[24–26]</sup>. Osteoblast differentiation and bone formation in *tg(sp7:egfp)* can be directly monitored. Our results also showed that the skull with green fluorescence in *tg(sp7:egfp)* can be directly observed using LSCM. Therefore, we selected 3–9 dpf wild-type AB strain and *tg(sp7:egfp)* zebrafish larvae to evaluate the protective actions of Sal B on osteogenesis in this study.

Dex is a common GC and is a recognized model drug for inducing GIO in mammals, such as rats and mice<sup>[35, 36]</sup>. Our data demonstrated that Dex caused a dose-dependent decrease in osteoblast differentiation and bone matrix mineralization in zebrafish larvae. *Runx2a*, *osteocalcin*, *ALP* and *osterix* are the main osteoblast-specific genes related to bone formation, which regulate osteoblastic differentiation and function<sup>[37]</sup>. Our study showed that Dex also down-regulated the mRNA expression of these osteoblast-specific genes in zebrafish larvae, which further confirmed that excessive Dex decreased osteogenesis by inhibiting osteoblast differentiation, mineralization and maturation. Excessive Dex can evoke osteoporosis by depressing osteoblastic bone formation in humans and higher vertebrates. Excess GC also inhibits osteoblast differentiation and bone nodule formation in bone marrow stroma stem cells<sup>[1]</sup>, consistent with our previous studies<sup>[16]</sup>. Further-

more, previous reports indicate that GC induces the inhibition of osteogenesis in zebrafish larvae<sup>[21]</sup>, consistent with our present results.

Sal B is the main pharmacologically active ingredient of approved drugs for cardio-cerebral vascular diseases. Our previous study<sup>[16, 18]</sup> showed that Sal B *in vitro* promoted bone marrow stromal cell differentiation into osteoblasts, increased osteoblast activity and decreased GC associated adipogenic differentiation. Moreover, an aqueous extract of *Radix Salviae miltiorrhizae*, of which the main ingredient is Sal B, prevented GC-induced bone loss<sup>[16]</sup>. Our data from this study showed that Sal B increased bone formation at concentrations ranging from 0.2 to 2  $\mu\text{mol/L}$  in a dose-dependent manner by promoting osteoblastic differentiation and bone matrix mineralization in zebrafish larvae, consistent with our previous findings *in vitro*<sup>[16, 18]</sup>. Importantly, Sal B ranging from 0.5 to 10.0  $\mu\text{mol/L}$  attenuated the decrease of osteoblast differentiation and bone matrix mineralization induced by Dex in a dose-dependent manner, particularly at 2  $\mu\text{mol/L}$ . Furthermore, Sal B also counteracted the down-regulation of osteoblast-specific gene expression triggered by Dex. Taken together, these results suggest that Sal B promotes osteogenesis at lower concentrations, and it may also prevent GC-induced inhibition of osteogenesis at relatively high concentrations in zebrafish larvae by stimulating osteoblast differentiation and bone mineralization. This finding is consistent with our previous report *in vitro*<sup>[16, 18]</sup>.

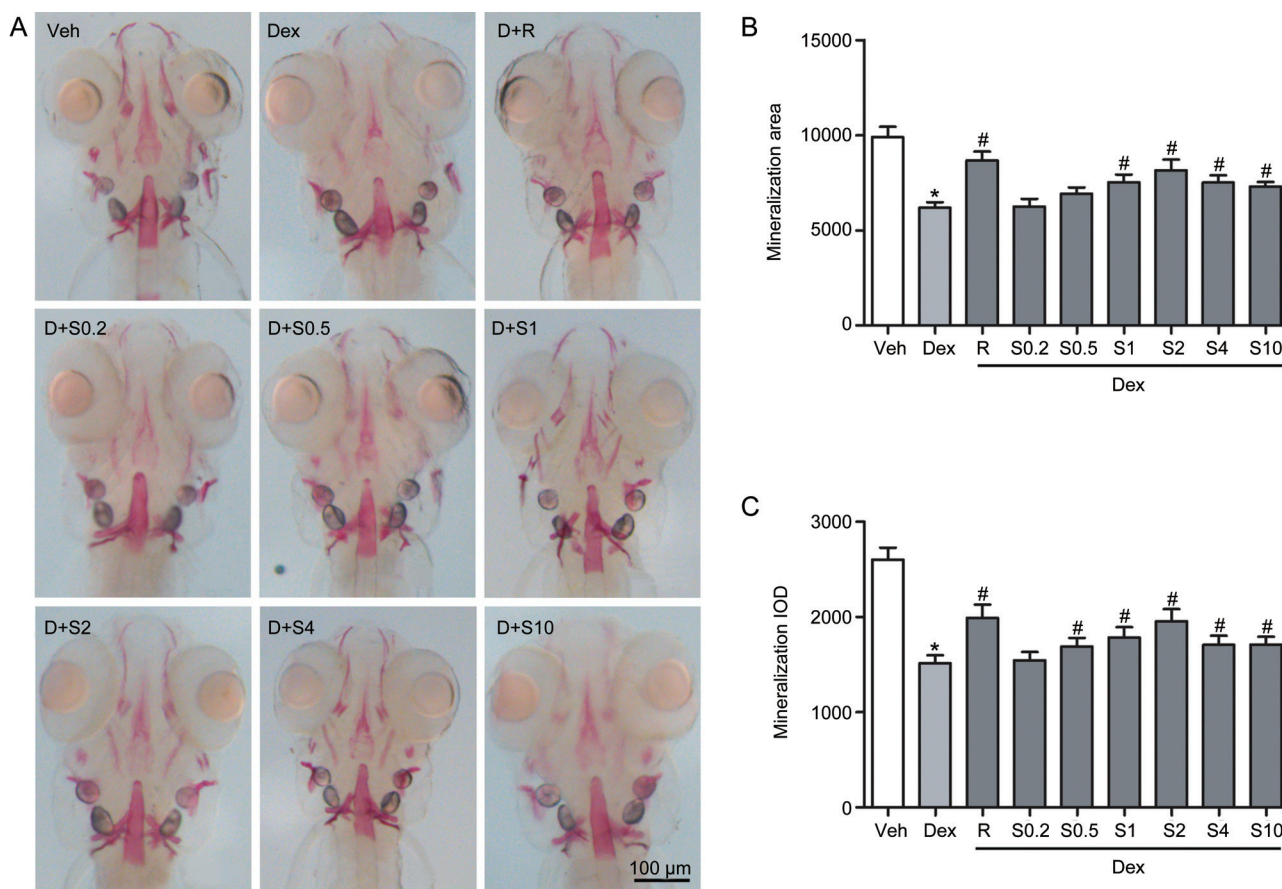


**Figure 6.** Sal B counteracts Dex-induced decrease of skull mineralization in AB strain larval zebrafish. (A) Dorsal view of skull stained by alizarin red in AB strain larval zebrafish at 9 dpf exposed to Dex ( $10 \mu\text{mol/L}$ ) in the presence or absence of Sal B for 6 d; (B) The effect of Sal B on skull mineralization area analyzed by IPP6.0 in 9 dpf zebrafish exposed to Dex; (C) The effect of Sal B on skull mineralization IOD analyzed by IPP6.0 in 9 dpf zebrafish exposed to Dex. Notes: IPP6.0 (Image-Pro Plus image analysis software version 6.0); IOD (integral optical density); Veh (vehicle control, 0.1% dimethyl sulphoxide); Dex (Dex  $10 \mu\text{mol/L}$ ); D+R (Dex+Rocalirol  $6 \times 10^{-6} \mu\text{g/mL}$ ); D+S0.2 (Dex+Sal B  $0.2 \mu\text{mol/L}$ ); D+S0.5 (Dex+Sal B  $0.5 \mu\text{mol/L}$ ); D+S1 (Dex+Sal B  $1 \mu\text{mol/L}$ ); D+S2 (Dex+Sal  $2 \mu\text{mol/L}$ ); D+S4 (Dex+Sal B  $4 \mu\text{mol/L}$ ); D+S10 (Dex+Sal B  $10 \mu\text{mol/L}$ ). Data are given as mean $\pm$ SD.  $n \geq 9$ . \* $P < 0.05$  vs vehicle control. # $P < 0.05$  vs Dex treatment.

Rocalirol, an effective bone-forming agent in clinical practice, is often used as a positive control anti-osteoporosis drug<sup>[38]</sup>. As is shown in our results (Figure 6), rocalirol at a concentration of  $6 \times 10^{-6} \mu\text{g/mL}$  increased bone mineralization and osteoblast differentiation in zebrafish larvae exposed to Dex, and the degree of increase in bone formation is similar to that of  $2 \mu\text{mol/L}$  Sal B. In addition, we found that rocalirol at concentrations from  $2 \times 10^{-6}$ – $10 \times 10^{-6} \mu\text{g/mL}$  showed a dose-dependent trend toward increased bone formation in larval zebrafish exposed to Dex, particularly at  $10 \times 10^{-6}$ . However, the larvae treated with rocalirol at concentrations of  $8 \times 10^{-6}$ – $10 \times 10^{-6} \mu\text{g/mL}$  had reduced swimming activity, malformation and death (data not shown). Interestingly, the larvae exposed to  $10 \mu\text{mol/L}$  Dex plus Sal B at concentrations ranging from  $0.2$  to  $10 \mu\text{mol/L}$  showed no decrease in swimming activity, malformation and death (data not shown). Together, these data suggest that Sal B may have protective effects on bone loss triggered by GC.

To clarify the mechanism by which Sal B attenuates GC-

induced osteogenesis inhibition, the levels of ROS and MDA were used as indicators of oxidation, and the activities of SOD, GSH and CAT were used as indicators of antioxidant levels in zebrafish exposed to  $10 \mu\text{mol/L}$  Dex in the presence or absence of  $2 \mu\text{mol/L}$  Sal B. Our study showed that Dex led to excessive ROS generation and increased MDA, whereas it inhibited the activity of SOD, GSH, and CAT in larval zebrafish, consistent with reports that GC is an oxidant stimulus that triggers ROS generation and activates OS in bone<sup>[13]</sup>. Sal B hampered the increase in ROS generation and MDA levels; however, it did not significantly increase the activities of these antioxidant enzymes. These results indicate that Sal B, as a natural potent antioxidant, directly clears ROS through its own antioxidant activity rather than by up-regulating endogenous antioxidant enzymes in zebrafish.

Both Sal B and tanshinol are strong natural antioxidants due to their phenolic hydroxyl groups<sup>[14, 15]</sup>, and Sal B can be transformed into tanshinol *in vivo*. Our previous study demonstrates that tanshinol not only stimulates osteoblast



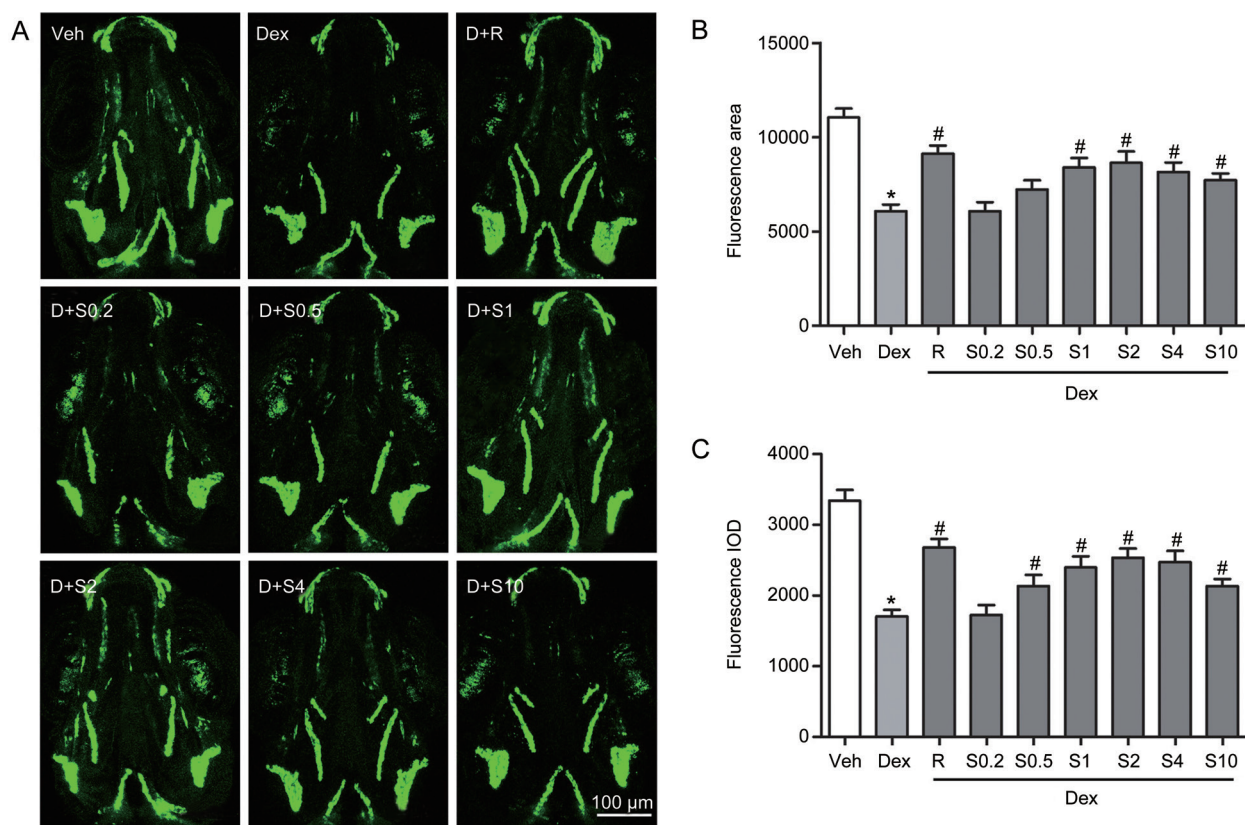


**Figure 7.** Sal B attenuated Dex-induced inhibition of skull osteoblasts differentiation in *tg(sp7:egfp)* larval zebrafish. (A) Green fluorescence images of skull dorsal aspect using LSCM in *tg(sp7:egfp)* larval zebrafish at 9 dpf exposure to Dex in the presence or absence of Sal B; (B) The effect of Sal B on green fluorescence area analyzed by IPP6.0 in 9-dpf *tg(sp7:egfp)* zebrafish exposed to Dex; (C) The effect of Sal B on green fluorescence IOD analyzed by IPP6.0 in 9-dpf *tg(sp7:egfp)* zebrafish exposed to Dex. Note: LSCM (laser scanning confocal microscopy); IPP6.0 (Image-Pro Plus image analysis software version 6.0); IOD (integral optical density); Veh (vehicle control, 0.1% dimethyl sulphoxide); Dex (Dex 10  $\mu\text{mol/L}$ ); D+R (Dex+Rocalirol 6 $\times 10^{-6}$   $\mu\text{g/mL}$ ); D+S0.2 (Dex+Sal B 0.2  $\mu\text{mol/L}$ ); D+S0.5 (Dex+Sal B 0.5  $\mu\text{mol/L}$ ); D+S1 (Dex+Sal B 1  $\mu\text{mol/L}$ ); D+S2 (Dex+Sal 2  $\mu\text{mol/L}$ ); D+S4 (Dex+Sal B 4  $\mu\text{mol/L}$ ); D+S10 (Dex+Sal B 10  $\mu\text{mol/L}$ ). Data are given as mean $\pm$ SD.  $n \geq 9$ . \* $P < 0.05$  vs vehicle control. # $P < 0.05$  vs Dex treatment.

differentiation and function<sup>[17]</sup> but also scavenges ROS triggered by  $\text{H}_2\text{O}_2$  and attenuates OS and OS-triggered inhibition of osteoblast differentiation by regulating *wnt/foxO3a/PPAR $\gamma$ / $\beta$ -catenin* signaling in  $\text{C}_2\text{C}_{12}$  cells<sup>[39]</sup>. Our previous finding showed that Sal B has beneficial effects on osteoblast growth, differentiation and mineralization *in vitro* by activating the expression of *Runx2* and  $\beta$ -catenin mRNA and decreasing the expression of *Dickkopf1* and *PPAR $\gamma$*  mRNA<sup>[17]</sup>. We found that Sal B counteracts the Dex-induced decreases in bone formation and osteoblast-specific gene expression in zebrafish larvae. In summary, our data reveal that Sal B attenuates GC-induced inhibition of osteogenesis, partially by removing ROS and reducing oxidative stress caused by GC.

In conclusion, this study demonstrated that Dex inhibited osteoblastic differentiation and bone mineralization, down-regulated osteoblastic-specific genes and increased ROS generation and the subsequent activation of OS in zebrafish larvae. Sal B attenuates these deleterious effects of Dex on bone formation in zebrafish larvae in part by scavenging excessive ROS and decreasing the oxidative stress elicited by Dex. Our findings support the further investigation of Sal B on bone

formation and indicate that Sal B may have protective effects against bone disorders, particularly GC-induced bone loss.

#### Acknowledgements

The authors are thankful to Dr Chung-der HSIAO's group from Chung Yuan Christian University, Taiwan, China for use of the *tg(sp7:egfp)* zebrafish. This research was supported by grants from the National Natural Science Foundation of China (81273518 and 31370824), the Science and Technology Planning Project of Guangdong Province (No 2012B060300027) and the Scientific Research Subject of Traditional Chinese Medicine Bureau of Guangdong Province (No 20152152).

#### Author contribution

Liao CUI, Shi-ying LUO, and Jing-jing ZHANG designed the research; Shi-ying LUO, Jing-feng CHEN, and Zhi-guo ZHONG performed the research; Xiao-hua LV and Ya-jun YANG contributed new analytical tools and reagents; Shi-ying LUO and Jing-feng CHEN analyzed data; and Shi-ying LUO, Liao CUI, Jing-jing ZHANG, and Ya-jun YANG wrote the paper.

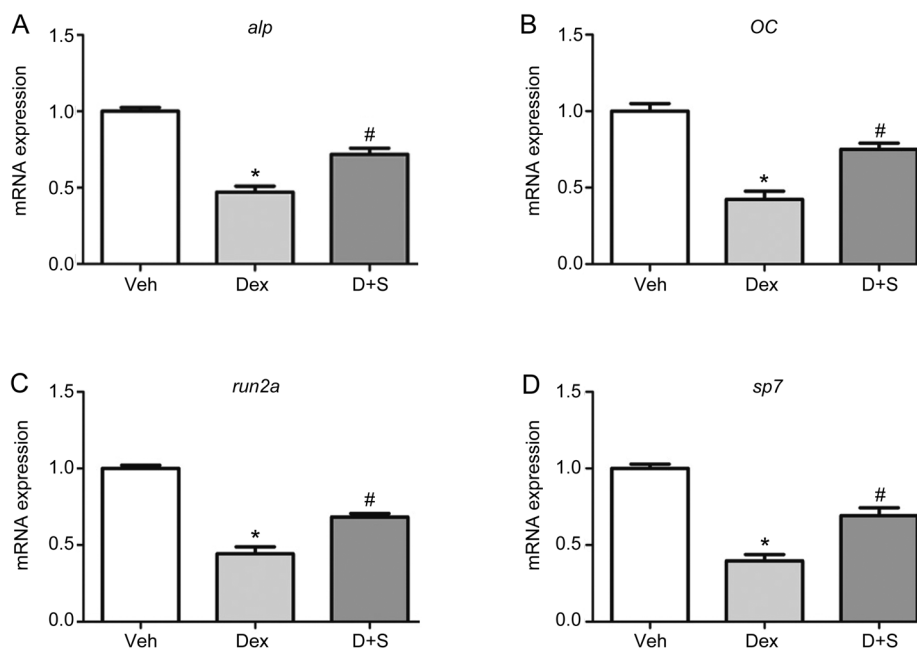


**Figure 8.** Sal B up-regulates the expressions of osteoblast-specific genes in larval zebrafish treated with Dex. Quantitative real-time PCR was performed to determine mRNA levels of (A) *alp*, (B) *OC*, (C) *runx2a* and (D) *sp7* genes. Note: Veh (vehicle control, 0.1% dimethyl sulphoxide); Dex (Dex 10 µmol/L); D+S (Dex+Sal B 2 µmol/L). Dates are given as mean±SEM of three independent experiments. \**P*<0.05 vs vehicle control. #*P*<0.05 vs Dex treatment.

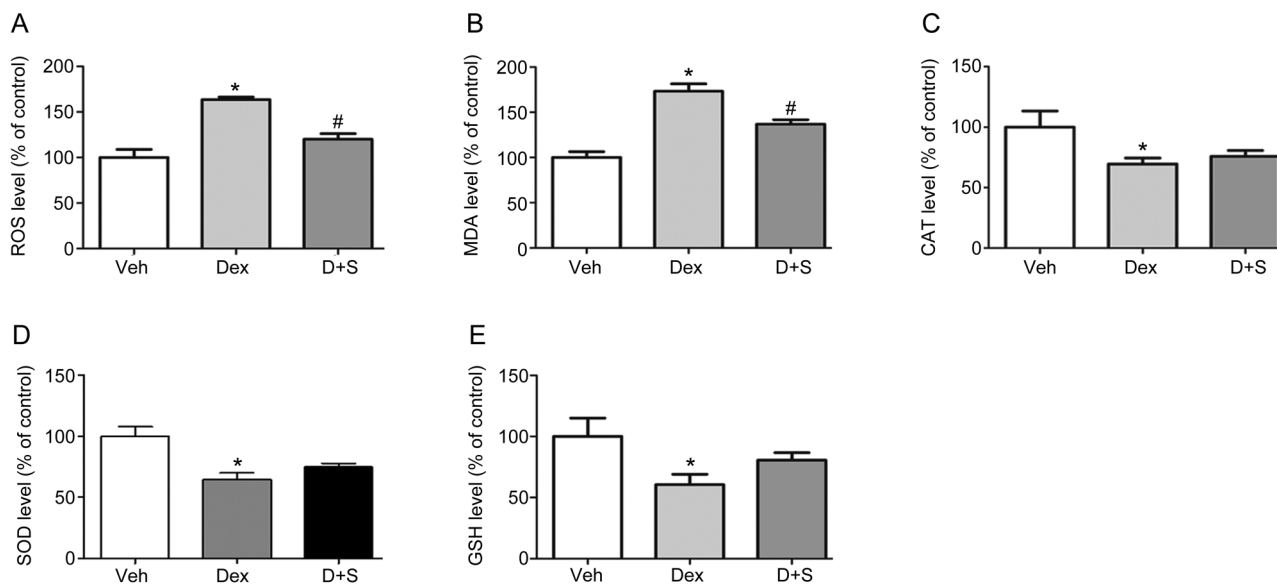


**Figure 9.** Sal B suppresses Dex-triggered oxidative stress in zebrafish larvae. (A) The level of ROS; (B) The level of MDA; (C) The activities of CAT; (D) The activities of SOD; (E) The activities of GSH. Note: Veh (vehicle control, 0.1% dimethyl sulphoxide); Dex (Dex 10 µmol/L); D+S (Dex+Sal B 2 µmol/L). Data are given as mean±SEM of three independent experiments. \**P*<0.05 vs vehicle control. #*P*<0.05 vs Dex treatment.

## References

- 1 Frenkel B, White W, Tuckermann J. Glucocorticoid-induced osteoporosis. *Adv Exp Med Biol* 2015; 872: 179–215.
- 2 Kaneko K, Kawai S. Mechanisms and therapeutics of glucocorticoid-induced osteoporosis. *Nihon Rinsho Meneki Gakkai Kaishi* 2011; 34: 138–48.
- 3 Sharma T, Islam N, Ahmad J, Akhtar N, Beg M. Correlation between bone mineral density and oxidative stress in postmenopausal women. *Indian J Endocrinol Metab* 2015; 19: 491–7.
- 4 Cervellati C, Bonaccorsi G, Cremonini E, Bergamini CM, Patella A, Castaldini C, et al. Bone mass density selectively correlates with serum markers of oxidative damage in post-menopausal women. *Clin*

- Chem Lab Med 2013; 51: 333–8.
- 5 Arslan A, Orkun S, Aydin G, Keles I, Tosun A, Arslan M, *et al*. Effects of ovariectomy and ascorbic acid supplement on oxidative stress parameters and bone mineral density in rats. *Libyan J Med* 2011; 6: doi: 10.3402/ljm.v6i0.5965.
  - 6 Muller FL, Lustgarten MS, Jang Y, Richardson A, Van Remmen H. Trends in oxidative aging theories. *Free Radic Biol Med* 2007; 43: 477–503.
  - 7 Huang CX, Lv B, Wang Y. Protein phosphatase 2A mediates oxidative stress induced apoptosis in osteoblasts. *Mediators Inflamm* 2015; 2015: 804260.
  - 8 Sato AY, Tu X, McAndrews KA, Plotkin LI, Bellido T. Prevention of glucocorticoid induced-apoptosis of osteoblasts and osteocytes by protecting against endoplasmic reticulum (ER) stress *in vitro* and *in vivo* female mice. *Bone* 2015; 73: 60–8.
  - 9 Shi J, Wang L, Zhang H, Jie Q, Li X, Shi Q, *et al*. Glucocorticoids: Dose-related effects on osteoclast formation and function via reactive oxygen species and autophagy. *Bone* 2015; 79: 222–32.
  - 10 Suda N, Morita I, Kuroda T, Murota S. Participation of oxidative stress in the process of osteoclast differentiation. *Biochim Biophys Acta* 1993; 1157: 318–23.
  - 11 Hurson CJ, Butler JS, Keating DT, Murray DW, Sadlier DM, O'Byrne JM, *et al*. Gene expression analysis in human osteoblasts exposed to dexamethasone identifies altered developmental pathways as putative drivers of osteoporosis. *BMC Musculoskelet Disord* 2007; 8: 12.
  - 12 Feng YL, Tang XL. Effect of glucocorticoid-induced oxidative stress on the expression of Cbfa1. *Chem Biol Interact* 2014; 207: 26–31.
  - 13 Almeida M, Han L, Ambrogini E, Weinstein RS, Manolagas SC. Glucocorticoids and tumor necrosis factor alpha increase oxidative stress and suppress Wnt protein signaling in osteoblasts. *J Biol Chem* 2011; 286: 44326–35.
  - 14 Chen CY, Li H, Yuan YN, Dai HQ, Yang B. Antioxidant activity and components of a traditional Chinese medicine formula consisting of *Crataegus pinnatifida* and *Salvia miltiorrhiza*. *BMC Complement Altern Med* 2013; 13: 99.
  - 15 Tang Y, Jacobi A, Vater C, Zou X, Stiehler M. Salvianolic acid B protects human endothelial progenitor cells against oxidative stress-mediated dysfunction by modulating Akt/mTOR/4EBP1, p38 MAPK/ATF2, and ERK1/2 signaling pathways. *Biochem Pharmacol* 2014; 90: 34–49.
  - 16 Cui L, Li T, Liu Y, Zhou L, Li P, Xu B, *et al*. Salvianolic acid B prevents bone loss in prednisone-treated rats through stimulation of osteogenesis and bone marrow angiogenesis. *PLoS One* 2012; 7: e34647.
  - 17 Cui L, Liu YY, Wu T, Ai CM, Chen HQ. Osteogenic effects of D+beta-3,4-dihydroxyphenyl lactic acid (salvianic acid A, SAA) on osteoblasts and bone marrow stromal cells of intact and prednisone-treated rats. *Acta Pharmacol Sin* 2009; 30: 321–32.
  - 18 Xu D, Xu L, Zhou C, Lee WY, Wu T, Cui L, *et al*. Salvianolic acid B promotes osteogenesis of human mesenchymal stem cells through activating ERK signaling pathway. *Int J Biochem Cell Biol* 2014; 51: 1–9.
  - 19 Goldsmith P. Zebrafish as a pharmacological tool: the how, why and when. *Curr Opin Pharmacol* 2004; 4: 504–12.
  - 20 Barros TP, Alderton WK, Reynolds HM, Roach AG, Berghmans S. Zebrafish: an emerging technology for *in vivo* pharmacological assessment to identify potential safety liabilities in early drug discovery. *Br J Pharmacol* 2008; 154: 1400–13.
  - 21 Barrett R, Chappell C, Quick M, Fleming A. A rapid, high content, *in vivo* model of glucocorticoid-induced osteoporosis. *Biotechnol J* 2006; 1: 651–5.
  - 22 Chen B, Yan YL, Liu C, Bo L, Li GF, Wang H, *et al*. Therapeutic effect of deferoxamine on iron overload-induced inhibition of osteogenesis in a zebrafish model. *Calcif Tissue Int* 2014; 94: 353–60.
  - 23 Jing LJ, Wang CM, Wei YJ, Jia XB, Xie L. Screening on antiosteoporotic active parts of dipsacus radix based on zebrafish model. *Zhong Yao Cai* 2014; 37: 635–40.
  - 24 Li N, Felber K, Elks P, Croucher P, Roehl HH. Tracking gene expression during zebrafish osteoblast differentiation. *Dev Dyn* 2009; 238: 459–66.
  - 25 DeLaurier A, Eames BF, Blanco-Sanchez B, Peng G, He X, Swartz ME, *et al*. Zebrafish sp7:EGFP: a transgenic for studying otic vesicle formation, skeletogenesis, and bone regeneration. *Genesis* 2010; 48: 505–11.
  - 26 Knopf F, Hammond C, Chekuru A, Hans S, Weber CW, Mahatma G, *et al*. Bone regenerates via dedifferentiation of osteoblasts in the zebrafish fin. *Dev Cell* 2011; 20: 713–24.
  - 27 Westerfield M. *The zebrafish book*. Oregon: University of Oregon Press; 2000.
  - 28 Walker MB, Kimmel CB. A two-color acid-free cartilage and bone stain for zebrafish larvae. *Biotech Histochem* 2007; 82: 23–8.
  - 29 Fleming A, Sato M, Goldsmith P. High-throughput *in vivo* screening for bone anabolic compounds with zebrafish. *J Biomol Screen* 2005; 10: 823–31.
  - 30 Ali S, Champagne DL, Spaink HP, Richardson MK. Zebrafish embryos and larvae: a new generation of disease models and drug screens. *Birth Defects Res C Embryo Today* 2011; 93: 115–33.
  - 31 Haga Y, Dominique VR, Du SJ. Analyzing notochord segmentation and intervertebral disc formation using the *twhh:gfp* transgenic zebrafish model. *Transgenic Res* 2009; 18: 669–83.
  - 32 Mork L, Crump G. Zebrafish craniofacial development: a window into early patterning. *Curr Top Dev Biol* 2015; 115: 235–69.
  - 33 Witten PE, Hansen A, Hall BK. Features of mono- and multinucleated bone resorbing cells of the zebrafish *Danio rerio* and their contribution to skeletal development, remodeling, and growth. *J Morphol* 2001; 250: 197–207.
  - 34 Sharif F, de Bakker MA, Richardson MK. Osteoclast-like cells in early Zebrafish embryos. *Cell J* 2014; 16: 211–24.
  - 35 Hui R, Liang D, Jiang X, Tang J, Cui J, Wei Q, *et al*. Variance of spinal osteoporosis induced by dexamethasone and methylprednisolone and its associated mechanism. *Steroids* 2015; 102: 65–75.
  - 36 Zheng G, Zhang X, Meng Q, Gong W, Wen X, Xie H. Protective effect of total isoflavones from *Pueraria lobata* on secondary osteoporosis induced by dexamethasone in rats. *Zhong Yao Cai* 2002; 25: 643–6.
  - 37 Thamamongood TA, Furuya R, Fukubas M, Nakamura M, Suzuki N, Hattori A. Expression of osteoblastic and osteoclastic genes during spontaneous regeneration and autotransplantation of goldfish scale: a new tool to study intramembranous bone regeneration. *Bone* 2012; 50: 1240–9.
  - 38 Matsumoto T, Endo I. Eldecacitol for the treatment of osteoporosis. *Drugs Today* 2012; 48: 189–96.
  - 39 Yang Y, Su Y, Wang D, Chen Y, Wu T, Li G, *et al*. Tanshinol attenuates the deleterious effects of oxidative stress on osteoblastic differentiation via Wnt/FoxO3a signaling. *Oxid Med Cell Longev* 2013; 2013: 351895.